

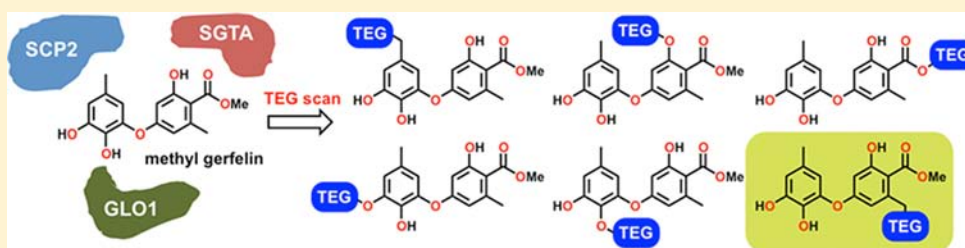
Dual Structure–Activity Relationship of Osteoclastogenesis Inhibitor Methyl Gerfelin Based on TEG Scanning

Naoki Kanoh,^{*,†} Takahiro Suzuki,[†] Makoto Kawatani,[‡] Yasuhiro Katou,[†] Hiroyuki Osada,[‡] and Yoshiharu Iwabuchi[†]

[†]Graduate School of Pharmaceutical Sciences, Tohoku University, 6-3 Aza-aoba, Aramaki, Aoba-ku, Sendai 980-8578, Japan

[‡]Chemical Biology Core Facility, RIKEN Advanced Science Institute, 2-1 Hirosawa, Wako, Saitama 351-0198, Japan

S Supporting Information



ABSTRACT: Methyl gerfelin derivatives, each having an amine-terminated tri(ethylene glycol) linker at the peripheral position, were designed and systematically synthesized. These “TEGylated” derivatives were then subjected to a structure–activity relationship (SAR) study to examine their glyoxalase 1-inhibition activity and binding affinity toward the three binding proteins identified. Among the derivatives synthesized, that with a NH₂-TEG linker at the C6-methyl group showed the most potent glyoxalase 1-inhibiting activity and glyoxalase 1 selectivity. These results indicated that derivatization at the C6-methyl group would be suitable for the further development of selective glyoxalase 1 inhibitors.

INTRODUCTION

Osteoclast-targeting small molecule inhibitors are useful not only for carrying out basic research on osteoclasts, but also for treating bone-related diseases, including osteoporosis, rheumatoid arthritis, and cancer bone metastasis.^{1,2} To date, many synthetic compounds and natural products have been reported to inhibit the differentiation and function of osteoclasts, and identification of the mechanisms underlying the inhibiting activity have deepened our understanding of osteoclast function.

In efforts to identify new small molecule inhibitors of osteoclast function, we found in 2008 that a fungal-derived natural product gerfelin (1)^{3,4} and its methyl ester methyl gerfelin (2) inhibited osteoclast differentiation *in vitro* (Figure 1A).⁵ Methyl gerfelin (2) suppressed osteoclastogenesis with an IC₅₀ value of 2.8 μM without affecting the survival and function of mature osteoclasts at the effective concentration.

To identify the cellular target(s) of methyl gerfelin (2) and the underlying inhibition mechanism, we prepared methyl gerfelin (2)-immobilized affinity beads by using a photo-cross-linking protocol.^{6,7}

Target protein “fishing” experiments using these methyl gerfelin-photo-cross-linked beads and peptide mass fingerprinting (PMF) analysis⁸ identified three cellular proteins as major methyl gerfelin-binding proteins: namely, glyoxalase 1 (GLO1),^{9,10} sterol binding protein 2 (SCP2),^{11,12} and small glutamine-rich tetratricopeptide repeat containing protein A (SGTA).¹³ On the basis of the subsequent biochemical and biological analysis, it was concluded that methyl gerfelin (2) inhibited GLO1 activity, resulting in an accumulation of methyl glyoxal that led to the inhibition of osteoclastogenesis.⁵ We also obtained the cocrystal structure of the methyl gerfelin (2)-GLO1 complex, which showed that a catechol moiety on ring A of methyl gerfelin (2) coordinates to the active site zinc ion of GLO1, while no significant interaction between ring B and GLO1 was observed.

Although we have thus obtained a detailed picture of GLO1 inhibition by methyl gerfelin (2), we still do not understand the binding mode between 2 and the other two binding proteins and the consequences of the interaction. It is now believed that small molecule drugs can act on multiple biomacromolecules, which in some cases can lead to not only sequestration of the drug from the main targets¹⁴ but also synergistic or adverse drug reactions.¹⁵ Thus, to fully understand the biological effects of methyl gerfelin (2) and to design more potent GLO1 and/or

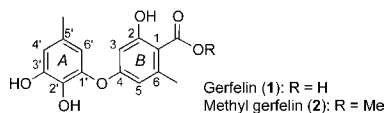


Figure 1. Structure of gerfelin and methyl gerfelin.

Received: July 5, 2012

Revised: December 14, 2012

Published: December 27, 2012

osteoclastogenesis inhibitors, the relationship between the gerfelin structure and GLO1-inhibiting activity as well as GLO1 selectivity over SCP2 and SGTA are of particular interest and remain to be clarified.

The first of these SAR studies (i.e., the study of the relation between GLO1 inhibition and M-GFN structure) can be easily performed by an enzyme inhibition assay of methyl gerfelin derivatives. However, the latter SAR study (that examining the relation between GLO1 selectivity and M-GFN structure) has to be done through an assay other than an enzymatic one, because the other two proteins are categorized in different classes and are not related to each other or to GLO1. An *in vitro* ligand-binding assay such as a pull-down experiment is a candidate, but would require a common functional group on every derivative in order to introduce the derivatives to affinity matrices, or to introduce a reporter group on the derivatives.

To address this issue, we propose herein a TEG scanning strategy, in which drug derivatives each having an amine-terminated tri(ethylene glycol) (NH₂-TEG) linker at a peripheral position are systematically prepared and tested in both functional and binding assays. The NH₂-TEG linker is designed to be used for two purposes: as a protruding area or a “bump” to assist in identifying the regions of a molecule that are important or unimportant for GLO1-inhibition activity, and as a “handle” to be introduced on affinity matrices for the pull-down experiments.

Thus, to gain insights into the SAR between GLO1-inhibition activity and GLO1-binding selectivity, we planned to apply this TEGylation strategy to methyl gerfelin (2). To this end, we designed and synthesized TEGylated methyl gerfelin (TMG) derivatives, and subjected them to GLO1-inhibition and protein pull-down assays. In addition, some of the TMG derivatives were subjected to an *in vitro* osteoclastogenesis inhibition assay. The results are reported in this article.

■ EXPERIMENTAL PROCEDURES

Materials and Methods. All reactions were carried out under an argon atmosphere with dehydrated solvents under anhydrous conditions, unless otherwise noted. Dehydrated THF and CH₂Cl₂ were purchased from Kanto Chemical Co., Inc. Other solvents were dehydrated and distilled according to standard protocols. Reagents were obtained from commercial suppliers and used without further purification, unless otherwise noted. The preparation of compounds **1**, **2**, **9**, **11**, **14**, **17**, **21**, **25**, and **39** was performed as described in the literatures those mentioned in the Results section. Compounds **26** and **36** are commercially available. The syntheses of compounds **10**, **12**, **15**, **16**, **18–20**, **22–24**, **27–35**, **37**, and **38** are described in the Supporting Information. Reactions were monitored by thin-layer chromatography (TLC) carried out on silica gel plates (Merck Kieselgel 60 F₂₅₄) or NH-silica gel plates (Fuji Silysia Chemical Co., Ltd.). Column chromatography was performed on silica gel 60N (spherical, neutral, 63–210 μ m; Kanto Chemical Co., Inc.). Flash column chromatography was performed on silica gel 60N (spherical, neutral, 40–50 μ m; Kanto Chemical Co., Inc.) or Chromatorex NHDM 1020 (NH₂-coated silica gel, 100–200 mesh; Fuji Silysia Chemical Co., Ltd.). All melting points were determined with a Yazawa Micro Melting Point BY-2 apparatus and were uncorrected. IR spectra were recorded on a JASCO FT/IR-410 spectrophotometer. ¹H NMR (400 MHz) and ¹³C NMR spectra (100 MHz) were recorded on JEOL JNM-AL-400 spectrometers, respectively. For ¹H NMR spectra, chemical

shifts (δ) are given from TMS (0.00 ppm) or CHCl₃ (7.26 ppm) in CDCl₃, or from CHD₂OD (3.30 ppm) in CD₃OD as internal standards. For ¹³C NMR spectra, chemical shifts (δ) are given from CDCl₃ (77.0 ppm) or CD₃OD (49.0 ppm) as internal standards. The following abbreviations were used to indicate the multiplicities: s = singlet, d = doublet, t = triplet, q = quartet, m = multiplet, br = broad. Mass spectra were recorded on JEOL JMS-DX303, JEOL JNM-AL500, and JEOL JMS-700 mass spectrometers.

Synthesis of TMG Compounds. Synthesis of TMG1 (3).

To a solution of ester **10** (88.0 mg, 0.256 mmol) in MeCN (2.1 mL) were added bromide **11** (66.5 mg, 0.213 mmol) and K₂CO₃ (162 mg, 1.17 mmol) at room temperature. After being stirred at reflux temperature for 13.5 h, the reaction mixture was filtered through a pad of Celite. The filtrate was concentrated under reduced pressure. The residue was purified by silica gel column chromatography (EtOAc/Hexane = 1/2 to 1/1) to give protected TMG1 (122 mg, 0.212 mmol, 100%) as a yellow oil.

Protected TMG1: IR (neat): 3383, 1715 cm⁻¹; ¹H NMR (400 MHz, CDCl₃): δ 6.45 (d, *J* = 2.0 Hz, 1H), 6.44 (d, *J* = 1.2 Hz, 1H), 6.39 (d, *J* = 2.0 Hz, 1H), 6.32 (d, *J* = 1.2 Hz, 1H), 5.04 (br s, 1H), 4.08 (t, *J* = 5.0 Hz, 2H), 3.87 (s, 3H), 3.81 (t, *J* = 5.0 Hz, 2H), 3.69 (t, *J* = 4.8 Hz, 2H), 3.60 (t, *J* = 4.6 Hz, 2H), 3.53 (t, *J* = 5.0 Hz, 2H), 3.31 (br q, *J* = 4.8 Hz, 2H), 2.24 (s, 3H), 2.23 (s, 3H), 1.66 (s, 6H), 1.44 (s, 9H); ¹³C NMR (100 MHz, CDCl₃): δ 168.2, 158.5, 157.1, 155.8, 149.1, 138.1, 137.4, 135.6, 131.6, 118.9, 118.5, 113.8, 110.7, 105.9, 99.8, 79.1, 70.9, 70.3, 70.3, 69.4, 68.8, 52.0, 40.4, 28.4, 25.8, 21.3, 19.7; HRMS (EI): calcd for C₃₀H₄₁O₁₀N (M⁺): 575.2730, found: 575.2753.

To a mixture of protected TMG1 (36 mg, 62.5 μ mol) in H₂O (0.25 mL) was added trifluoroacetic acid (TFA) (1.25 mL) at 0 °C. After being stirred at room temperature for 1 h, the reaction mixture was concentrated under reduced pressure. The residue was purified by silica gel column chromatography (MeOH/CHCl₃ = 1/9) to give TMG1 (**3**) (27.2 mg, 62.5 μ mol, 100%) as a yellow solid.

TMG1 (**3**): Mp. 43–44 °C; IR (neat): 3359, 3186, 1722 cm⁻¹; ¹H NMR (400 MHz, CDCl₃): δ 6.75 (d, *J* = 1.6 Hz, 1H), 6.57 (s, 1H), 6.28 (s, 1H), 6.24 (d, *J* = 1.6 Hz, 1H), 5.75–5.40 (br s, 4H), 4.21 (t, *J* = 4.4 Hz, 2H), 3.87 (s, 3H), 3.76 (t, *J* = 4.4 Hz, 2H), 3.63 (t, *J* = 4.0 Hz, 2H), 3.53 (t, *J* = 4.0 Hz, 2H), 3.45 (s, 2H), 2.78 (s, 2H), 2.19 (s, 6H); ¹³C NMR (100 MHz, CDCl₃): δ 168.7, 159.7, 158.1, 147.4, 142.4, 138.0, 135.2, 128.7, 118.4, 112.9, 112.0, 109.8, 101.2, 71.1, 70.6, 70.4, 70.4, 69.7, 52.0, 40.6, 20.8, 19.7; HRMS (EI): calcd for C₂₂H₂₉O₈N (M⁺): 435.1893, found: 435.1881.

Synthesis of TMG2 (4). To a mixture of amide **16** (6.45 mg, 11.5 μ mol) in H₂O (0.33 mL) was added TFA (1.0 mL) at 0 °C. After being stirred at room temperature for 3.5 h, the reaction mixture was concentrated under reduced pressure. The residue was purified by silica gel column chromatography (MeOH/CHCl₃ = 1/9 to 1/4) to give TMG2 (**4**) (4.80 mg, 11.4 μ mol, 99%) as a red solid.

TMG2 (**4**): Mp. 90–92 °C; IR (neat): 3065, 1577 cm⁻¹; ¹H NMR (400 MHz, CD₃OD): δ 7.87 (s, 1H), 6.47 (s, 1H), 6.25 (s, 1H), 6.22 (s, 2H), 3.62 (s, 2H), 3.64 (s, 4H), 3.54 (m, 4H), 2.84 (d, *J* = 4.0 Hz, 2H), 2.28 (s, 3H), 2.14 (s, 3H); ¹³C NMR (100 MHz, CD₃OD): δ 171.6, 161.0, 158.9, 148.1, 144.6, 139.7, 136.4, 129.9, 119.4, 113.8, 113.5, 110.6, 103.2, 79.4, 71.5, 71.3, 70.6, 41.5, 40.5, 20.9, 20.5; HRMS (EI): calcd for C₂₁H₂₈O₇N₂ (M⁺): 420.1897, found: 420.1890.

Synthesis of TMG3 (5). A solution of biaryl ether **27** (2.85 mg, 4.46 μ mol) in 1.25 M HCl/MeOH (1.0 mL) was stirred

under reflux for 18 h. The reaction mixture was concentrated under reduced pressure. The residue was purified by silica gel column chromatography (MeOH/CHCl₃ = 0/1 to 1/4) to give TMG3 (5) (2.0 mg, 4.46 μ mol, 99%) as an orange oil.

TMG3 (5): IR (neat): 3420, 1655 cm⁻¹; ¹H NMR (400 MHz, CDCl₃): δ 7.15 (s, 1H), 6.62 (s, 1H), 6.36 (s, 1H), 6.24 (s, 1H), 4.80 (s, 2H), 3.92 (s, 3H), 3.77–3.60 (m, 8H), 3.54 (br s, 2H), 2.84 (br s, 2H), 2.22 (s, 3H); ¹³C NMR (100 MHz, CDCl₃): δ 171.2, 165.4, 163.9, 147.7, 144.4, 141.7, 129.2, 113.8, 112.7, 107.5, 103.9, 101.8, 71.3, 70.7, 70.4, 70.2, 70.1, 52.0, 29.7, 20.9; HRMS (EI): calcd for C₂₂H₂₉NO₉ (M⁺): 451.1842, found: 451.1844.

Synthesis of TMG4 (6). To a solution of carbamate 28 (15.6 mg, 31.0 μ mol) in CH₂Cl₂ (1 mL) was added TFA (2.0 mL) at 0 °C. After being stirred at room temperature for 1 h, the reaction mixture was concentrated under reduced pressure. The residue was purified by silica gel column chromatography (MeOH/CHCl₃ = 1/20) to give TMG4 (6) (13.5 mg, 31.0 μ mol, 100%) as a red solid.

TMG4 (6): Mp. 98–99 °C; IR (neat): 3366, 1718, 1654 cm⁻¹; ¹H NMR (400 MHz, CDCl₃): δ 6.63 (d, *J* = 1.4 Hz, 1H), 6.36 (d, *J* = 1.4 Hz, 1H), 6.33 (d, *J* = 2.2 Hz, 1H), 6.31 (d, *J* = 2.2 Hz, 1H), 4.02 (t, *J* = 4.2 Hz, 2H), 3.93 (s, 3H), 3.69–3.62 (m, 6H), 3.54 (t, *J* = 4.8 Hz, 2H), 2.88 (t, *J* = 5.0 Hz, 2H), 2.49 (s, 3H), 2.23 (s, 3H); ¹³C NMR (100 MHz, CDCl₃): δ 172.0, 165.0, 162.6, 151.5, 147.1, 143.5, 136.3, 134.9, 114.6, 113.5, 111.7, 106.7, 102.0, 73.0, 73.0, 70.3, 69.8, 69.6, 51.9, 41.3, 24.3, 21.1; HRMS (EI): calcd for C₂₂H₂₉O₈N (M⁺): 435.1893, found: 435.1848.

Synthesis of TMG5 (7). To a solution of carbamate 29 (9.0 mg, 16.8 μ mol) in CH₂Cl₂ (1 mL) was added TFA (1 mL) at 0 °C. After being stirred at room temperature for 1 h, the reaction mixture was concentrated under reduced pressure. The residue was purified by silica gel column chromatography (MeOH/CHCl₃ = 1/20) to give TMG5 (7) (7.3 mg, 16.8 μ mol, 100%) as a red solid.

TMG5 (7): Mp. 39–40 °C; IR (neat): 3363, 1719, 1652 cm⁻¹; ¹H NMR (400 MHz, CDCl₃): δ 6.55 (d, *J* = 1.2 Hz, 1H), 6.50 (d, *J* = 1.2 Hz, 1H), 6.41 (d, *J* = 2.2 Hz, 1H), 6.24 (d, *J* = 2.2 Hz, 1H), 4.15 (t, *J* = 4.4 Hz, 2H), 3.91 (s, 3H), 3.86 (t, *J* = 4.4 Hz, 2H), 3.67 (s, 4H), 2.81 (t, *J* = 5.0 Hz, 2H), 2.48 (s, 3H), 2.24 (s, 3H); ¹³C NMR (100 MHz, CDCl₃): δ 172.1, 165.1, 163.1, 148.3, 143.2, 142.2, 138.1, 127.9, 116.1, 112.1, 111.1, 106.1, 101.5, 72.4, 70.7, 69.7, 69.5, 68.6, 51.8, 40.8, 24.3, 21.0; HRMS (EI): calcd for C₂₂H₂₉O₈N (M⁺): 435.1893, found: 435.1877.

Synthesis of TMG6 (8). To a solution of phenol 35 (15.4 mg, 48.4 μ mol) in MeOH (484 μ L) were added amine (36) (21.5 mg, 145 μ mol), AcOH (22 μ L, 387 μ mol), and NaBH₃CN (12.2 mg, 194 μ mol) at room temperature. After being stirred at room temperature for 39 h, the reaction mixture was concentrated and purified by silica gel column chromatography (MeOH/CHCl₃ = 0/1 to 1/9 to 1/4) to give TMG6 (8) (19.7 mg, 43.7 μ mol, 90%) as a brown solid.

TMG6 (8): Mp. 63–64 °C; IR (neat): 3023, 1651 cm⁻¹; ¹H NMR (400 MHz, CD₃OD): δ 6.70 (s, 1H), 6.50 (s, 1H), 6.36 (d, *J* = 2.4 Hz, 1H), 6.17 (d, *J* = 2.4 Hz, 1H), 3.91 (s, 3H), 3.66 (br s, 1H), 3.61 (br s, 1H), 3.56 (t, *J* = 5.0 Hz, 2H), 2.89 (t, *J* = 5.2 Hz, 2H), 2.79 (t, *J* = 5.0 Hz, 2H), 2.44 (s, 3H); ¹³C NMR (100 MHz, CD₃OD): δ 173.0, 165.2, 164.0, 149.6, 143.9, 143.5, 139.7, 130.3, 113.8, 113.7, 112.6, 108.7, 102.6, 72.3, 71.2, 70.5, 58.3, 53.7, 52.3, 41.7, 23.9, 18.4; HRMS (FAB): calcd for C₂₂H₃₁O₈N₂ (M⁺+H): 451.2080, found: 451.2087.

Preparation of TMG-Immobilized Beads. Commercially available Affi-Gel 10 (20 μ mol NHS/mL of gel; BIO-RAD) beads were washed twice with Milli-Q (volume of Milli-Q to volume of beads = 4:1) at room temperature. To the swelled beads (200 μ L) were added a solution of TMG compound (20 μ mol) in coupling solution (1:1 dioxane/0.1 M aq. NaHCO₃, 300 μ L) and MeOH (2 \times 120 μ L) at room temperature. The mixture was shaken at the same temperature for 2 h. The resultant beads were washed with MeOH (5 \times 900 μ L). To the beads was added a 1 M solution of ethanolamine in Tris-HCl buffer (0.1 M Tris-HCl, pH 8.0, 1 mL), and the mixture was shaken for another 1 h. The beads were transferred into a spin column using Milli-Q (4 \times 400 μ L). The beads were washed successively with MeOH, DMSO, MeOH, and PBS buffer (137 mM NaCl, 3 mM KCl, 9 mM NaHPO₄, 1.5 mM KH₂PO₄, pH 7.4, 3 \times 400 μ L each). The beads were suspended in PBS buffer containing 1 mM sodium azide, and stored at 4 °C. The beads were washed with PBS prior to use.

Expression and Purification of His-Tagged Proteins. BL21 (DE3) pLysS *E. coli* cells expressing each of the His-tagged proteins were grown in LB media (0.5% Bacto-Yeast Extract, 1% Bacto-Tryptone, 1% NaCl) containing 100 mg/L ampicillin with shaking at 37 °C until the OD₆₀₀ reached 0.2. The cells were then incubated with 0.1 mM IPTG for 4 h and harvested by centrifugation at 2000g at 4 °C for 5 min. After cell lysis by homogenization with a syringe and sonication, the insoluble material was removed by centrifugation at 22 000g at 4 °C for 30 min, and the supernatant was collected as a cell lysate. Each His-tagged protein was purified on a Ni Sepharose 6 Fast Flow column (GE Healthcare) according to the manufacturer's instructions.

In Vitro GLO1-Inhibition Assay. Kinetic measurements were carried out by using a Microplate Reader (BioTek Synergy Mx) to monitor the increase in absorbance at 240 nm originating from the formation of S-D-lactoylglutathione (ϵ_{240} = 3.37 mM⁻¹cm⁻¹) at 30 °C. After the reaction buffer (0.1 M sodium phosphate, 14.6 mM MgSO₄, 1 mM glutathione, 8 mM methylglyoxal, pH 7.0) was preincubated at 30 °C for 5 min, the reaction was initiated by the addition of His-GLO1 (24 ng) with or without compound.

Detection of His-SGTA, His-GLO1, and His-SCP2 by Using TMG Beads. The TMG beads were incubated in binding buffer (10 mM Tris-HCl, 50 mM KCl, 5 mM MgCl₂, 1 mM EDTA, pH 7.6) containing His-SGTA (68 μ g), His-GLO1 (40 μ g), His-SCP2 (30 μ g), 0.1% Triton X-100, and a protease inhibitor mixture (Roche) (total 700 μ L) at 4 °C for 4.5 h on a rotator. The reacted TMG beads were washed with binding buffer containing 0.1% Triton X-100 (7 \times 1 mL) followed by binding buffer alone (3 \times 1 mL). Twenty microliters of the SDS sample buffer (125 mM Tris-HCl, 10% 2-mercaptoethanol, 4% SDS, 20% glycerol, 0.004% bromophenol blue, pH 6.8) was added to the washed beads and the bound proteins were eluted by boiling at 110 °C for 5 min. The eluted proteins were separated by SDS-PAGE and visualized by CBB staining.

Detection of Endogenous SGTA, GLO1, and SCP2 Using TMG Beads. RAW264.7 cells were harvested and washed twice with PBS buffer (137 mM NaCl, 3 mM KCl, 9 mM NaHPO₄, 1.5 mM KH₂PO₄, pH 7.4), then resuspended in binding buffer containing 0.1% Tween 20 and protease inhibitor mixture (Roche). The washed cells were homogenized with a syringe and sonicated. Insoluble materials were removed by centrifugation at 22 000g at 4 °C for 30 min, and the supernatant was collected as cell lysate. After the cell lysate (4

mg total protein) was precleared by incubation with control beads (20 μ L) at 4 $^{\circ}$ C for 1 h, it was incubated with TMG beads (20 μ L) at 4 $^{\circ}$ C for 12.5 h. The reacted TMG beads were washed with binding buffer containing 0.1% Triton X-100 (7 \times 1 mL) followed by binding buffer alone (3 \times 1 mL). The bound proteins were eluted with SDS sample buffer, separated by SDS-PAGE, and transferred to PVDF membrane. After the membrane was treated with monoclonal primary antibodies against SGTA (sc-100875, Lot# K1710; Santa Cruz Biotech Inc.) followed by a HRP-conjugated antimouse IgG polyclonal secondary antibody (Santa Cruz Biotech Inc.), or polyclonal primary antibodies against GLO1 (sc-67351, Lot# G0208; Santa Cruz Biotech Inc.) followed by a HRP-conjugated antirabbit IgG polyclonal secondary antibody (Zymed) or polyclonal primary antibodies against SCP2 (sc-32835, Lot# D1510; Santa Cruz Biotech Inc.) followed by a HRP-conjugated antigoat IgG polyclonal secondary antibody (Santa Cruz Biotech Inc.), the immune complexes were detected with SuperSignal West Dura Extended Duration substrate (Thermo Scientific) according to the manufacturer's instructions.

Osteoclastogenesis Suppression Assay. The osteoclastogenesis suppression assay was performed as described in the literature.⁵ Briefly, mouse bone marrow-derived macrophages (BMM) were treated with various concentrations of TMG compound in the presence of the receptor activator of the NF- κ B ligand (RANKL) and macrophage colony stimulating factor (M-CSF) for 72 h. Cells were fixed and stained for tartrate-resistant acid phosphatase (TRAP), and TRAP-positive multinucleated cells were counted.

RESULTS AND DISCUSSION

Design and Synthesis of TEGylated Methyl Gerfelin Derivatives. We designed six TEGylated methyl gerfelin derivatives (TMG1–6: 3–8) with an NH₂-TEG linker on the peripheral groups of the methyl gerfelin molecule: i.e., on the C1-carboxyl group, C6- and C5'-methyl groups, and C2-, C2', C3'-hydroxyl groups (Figure 2).¹⁶ The introduction of an NH₂-TEG unit at each of the above-mentioned positions except for C6-methyl was thought to be possible via an appropriately protected methyl gerfelin. In particular, we expected that benzylic radical halogenation would be suitable for derivatiza-

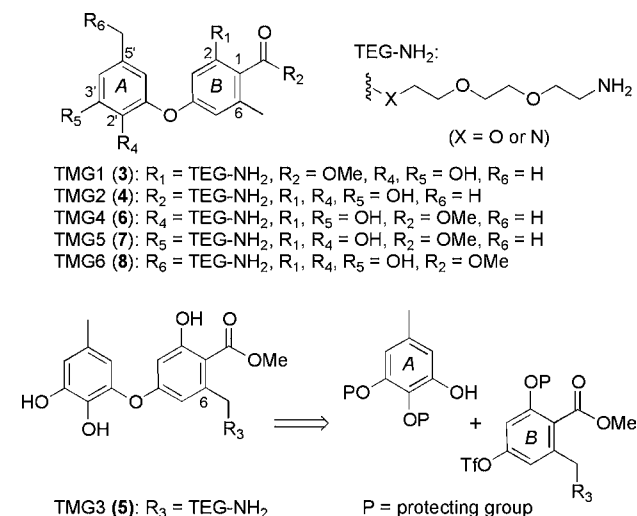
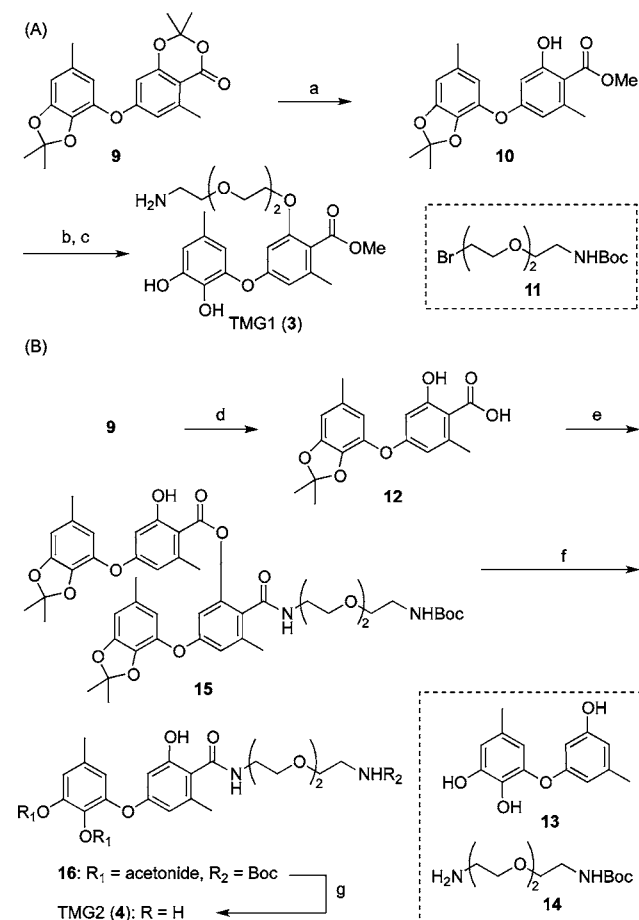


Figure 2. Design of TEGylated methyl gerfelin derivatives.

tion at the C5'-methyl group adjacent to the electron-rich A ring. In contrast, we considered that the selective halogenation of the C6-methyl group in the presence of the C5'-methyl group would not be straightforward; we therefore planned to derivatize the C6-methyl group before the coupling of the A and B rings.

Synthesis of TEGylated Methyl Gerfelin Derivatives. Synthesis of TMG1 (3) began with gerfelin diacetone (9), a synthetic intermediate of Watanabe's first total synthesis¹⁷ of methyl gerfelin (2) (Scheme 1A). After trans-esterification of 9, the resulting phenol 10 was coupled with a known bromide 11,¹⁸ and global deprotection using TFA provided TMG1 (3) in 97% yield in three steps.

Scheme 1. Synthesis of TMG1 (3) and TMG2 (4)



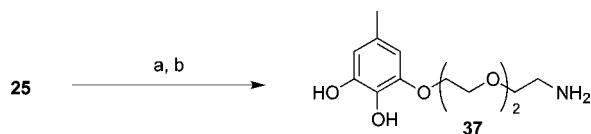
Reagents and conditions: (a) MeONa, MeOH, rt, 10 h, 97%; (b) 11, K₂CO₃, MeCN, reflux, 13.5 h, 100%; (c) TFA-H₂O (5:1), rt, 1 h, 100%; (d) KOH, THF-H₂O (1:1), reflux, 6 h, 100%; (e) 12, EDCI, DMAP, CH₂Cl₂, rt, 24 h, 55% from 14; (f) KOH, THF-H₂O (1:1), 50 $^{\circ}$ C, 1 h, 95%; (g) TFA-H₂O (3:1), rt, 1 h, 99%. TFA = trifluoroacetic acid, THF = tetrahydrofuran, EDCI = 1-ethyl-3-(3-dimethylaminopropyl)carbodiimide hydrochloride, DMAP = 4-(dimethylamino)pyridine.

For the synthesis of TMG2 (4), gerfelin diacetone (9) was first converted to carboxylic acid 12 via alkali hydrolysis in quantitative yield (Scheme 1B). Acid hydrolysis of 9 (TFA, H₂O, 95 $^{\circ}$ C) quantitatively led to the decarboxylated product 13 instead. Treatment of carboxylic acid 12 with amine 14 in the presence of EDCI and DMAP afforded the pseudodimeric amide 15 in 55% yield from 14, which was then hydrolyzed

with TBAF to give aldehyde **35**. Reductive coupling of **35** and diamine **36** using NaBH_3CN and AcOH proceeded smoothly to give the desired TMG6 (**8**) in 90% yield.

Synthesis of the Gelfelin A Ring Derivative. In addition to TMG1–6, a methyl gelfelin A ring derivative was designed and synthesized to verify the importance of the B ring for the GLO1-inhibiting activity. To this end, the protected phenol **25** was coupled with bromide **11** and the following global deprotection gave the A ring derivative **37** in 88% yield in 2 steps (Scheme 5).

Scheme 5. Synthesis of the Gelfelin A Ring Derivative



Reagents and conditions: (a) **11**, NaI , K_2CO_3 , MeCN , reflux, 24 h, 95%; (b) $\text{TFA-H}_2\text{O}$ (4:1), rt, 2 h, 93%.

In Vitro GLO1 Inhibition of TMG Compounds and Other Derivatives. With the desired TMG compounds and their synthetic intermediates in hand, the *in vitro* GLO1-inhibitory activities of these compounds were determined according to the protocol reported by Oray et al.¹⁹ The structures of the compounds and their IC_{50} values are summarized in Figure 3.

Among the TMG compounds, TMG1, TMG2, and TMG3 were found to retain GLO1-inhibitory activity. TMG3 showed inhibitory activity ($0.78 \pm 0.17 \mu\text{M}$) comparable to those of methyl gelfelin (**2**) and gelfelin (**1**). This result indicates that the functionalization at the C6-methyl group had almost no effect on the interaction with, and thus the inhibition of, GLO1. As seen in TMG1 and TMG2, introduction of an NH_2 -TEG linker at the C1 carbonyl and C2 hydroxyl groups had some effect, increasing the IC_{50} value up to 2-fold that of the parent molecule. In contrast, TMG4 and TMG5, each of which had a linker at the C2' or C3' hydroxyl groups, respectively, almost lost their GLO1-inhibitory activity. Introduction of a methyl group or acetonide at the same position also had the same effect (see compounds **9**, **30**, and **31**). TMG6 having a linker at the C5' methyl also lost its GLO1-inhibitory activity. Indeed, modification of the C5' methyl group tends to lower the biological activity. The observed rank order of C5'-methyl modification for GLO1-inhibitory activity was methyl (parent compound **2**) > aldehyde (**35**) > hydroxyl (**38**) > TEG- NH_2 linker (**8**).

Overall, these results are mostly consistent with the X-ray structure of GLO1 complexed with methyl gelfelin: the methoxycarbonyl group in the B ring of **2** points outward from the substrate-binding pocket of GLO1, whereas the C5'-methyl group is placed in the deep pocket of the substrate-binding site with the C2'- and C3'-hydroxyl groups bound to the Zn catalytic center of GLO1. However, it should be emphasized that the GLO1-inhibitory activity of decarboxylated compound **13**, as well as that of the A ring derivatives **37** and **39**, was quite low. This means that, although no interaction between the B ring unit and GLO1 was observed in the cocrystal structure,⁵ the presence of the B ring unit is quite important for the biological activity of these derivatives. Also, the loss of biological activity in the C2'- and C3'-O-TEGylated and methylated derivatives (TMG4, TMG5, **30** and **31**)

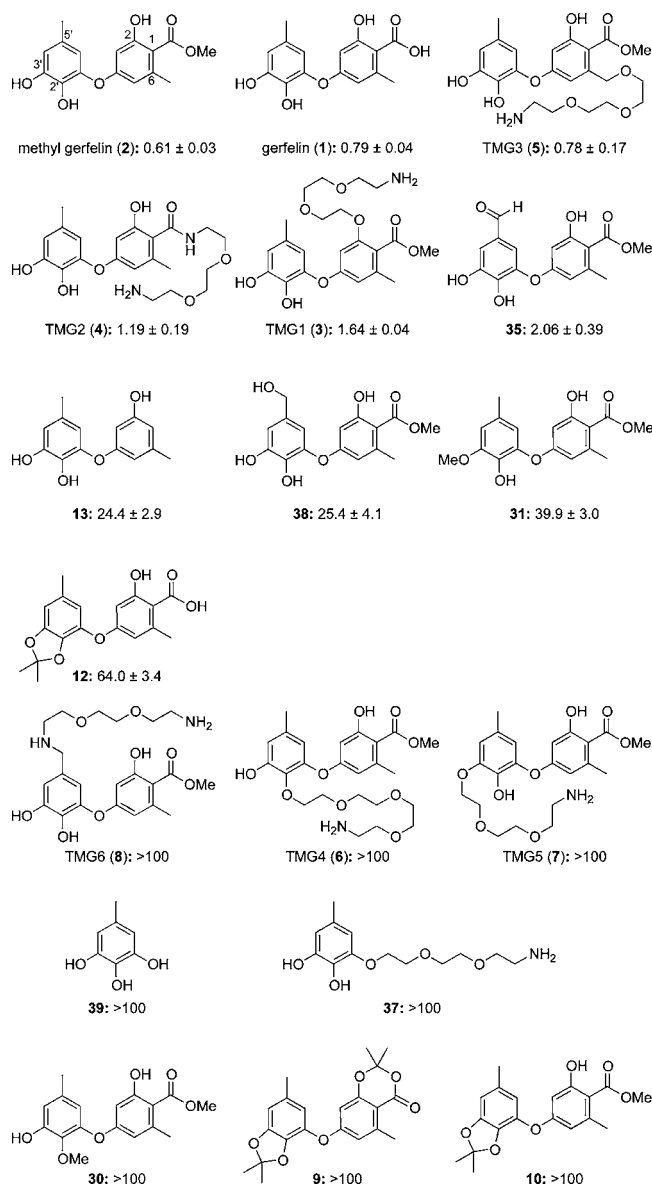


Figure 3. *In vitro* GLO1-inhibition activity of TMG compounds and other derivatives. IC_{50} values are reported in μM . The compounds are placed in a left-to-right direction in order of decreasing GLO1-inhibition activity.

indicated that both phenolic hydroxyl groups have to be in an unprotected form to exert GLO1 inhibition.

Preparation of TMG Beads. Next, to estimate the selectivity of TMG compounds toward the three binding proteins, the compounds were introduced on affinity matrices and subjected to competitive pull-down experiments. The TMG compound-introduced affinity beads (TMG beads) were prepared as follows: Swelled NHS-activated Affi-Gel 10 beads were treated with each TMG compound in 0.1 M aq. NaHCO_3 -dioxane (1:1), and the resultant beads were blocked with ethanolamine and washed successively to afford TMG1–6 beads (Figure 4A). The amount of TMG molecules introduced on the affinity beads was estimated to be $3.69 \pm 0.11 \text{ nmol}/\mu\text{L}$.²⁰ Control affinity beads were also prepared in the same manner.

Protein-Binding Property of Each TMG. Each TMG bead was independently combined with a mixed solution of

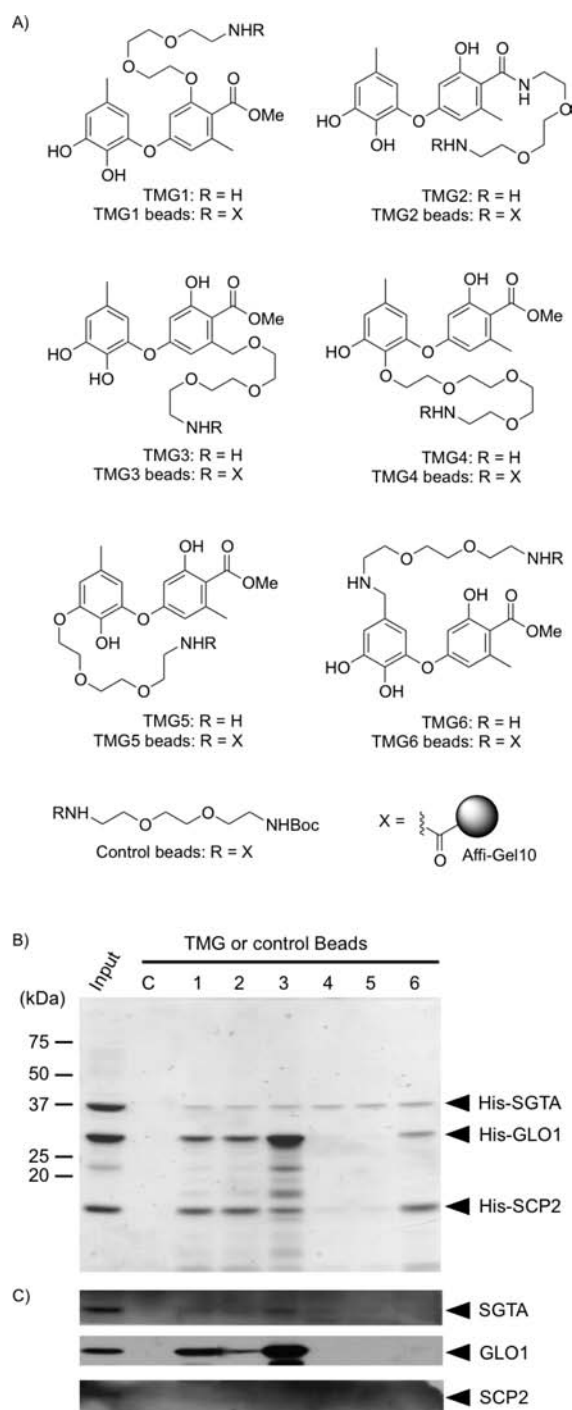


Figure 4. Protein-binding property of each TMG bead. (A) Structure of TMG compounds and TMG beads. (B,C) Pull-down assay using TMG beads. Control beads or each type of TMG bead was independently combined with a mixed solution of His-SGTA, His-GLO1, and His-SCP2 (B), or with RAW264.7 cell lysate (C). The separated bead-bound proteins were visualized by CBB staining (B) or Western blotting (C). C: control.

three purified (His)₆-tagged recombinant proteins, and the bead-bound proteins were separated using SDS-PAGE and visualized using CBB staining (Figure 4B).

All three proteins were found to bind to the TMG beads but not to the control beads, indicating that the proteins bind to the methyl gerfelin portion. The (His)₆-SGTA protein was found to bind to all TMG compounds to a similar extent. It was

assumed from this result that SGTA loosely recognizes and binds to aromatic ring(s) of methyl gerfelin (2). On the other hand, the (His)₆-GLO1 protein was found to bind selectively to TMG1-, TMG2-, TMG3-, and TMG6 beads. Among these beads, the TMG3 beads exhibited the best binding activity toward the (His)₆-GLO1 protein. The binding profile of TMG beads to the (His)₆-SCP2 protein was quite similar to that to the (His)₆-GLO1 protein, suggesting that GLO1 and SCP2 recognize and bind to almost the same region of the surface of methyl gerfelin (2). However, in contrast to (His)₆-GLO1, the amount of (His)₆-SCP2 protein bound to TMG3 beads did not increase. These results indicate that TMG3 had better selectivity toward GLO1 than did SGTA and SCP2. We performed the binding experiments with each of the three purified proteins, and almost the same results were obtained (data not shown).

Pull-down experiments utilizing cell lysate of RAW264.7 cells instead of purified proteins were also carried out (Figure 3C). Each TMG bead was independently incubated with the cell lysate of RAW264.7 cells, and the bound proteins were resolved with SDS-PAGE and detected by Western blot analysis. Again, TMG3 beads precipitated endogenous GLO1 more efficiently than other TMG beads. Only low levels of binding with endogenous SGTA and SCP2 were detected in these cases, suggesting the superior selectivity of TMG3. From these experiments, we concluded that TMG3 is a selective binder and inhibitor of GLO1.

Osteoclastogenesis Suppression of TMG Compounds.

The levels of *in vitro* osteoclastogenesis inhibition activity of TMG1, TMG3, and TMG4 were determined by cellular phenotype-based screening using mouse bone marrow-derived macrophages (BMMs). Briefly, BMMs were treated with test compounds for three days in the presence of the receptor activator of the NF- κ B ligand (RANKL) and macrophage colony stimulating factor (M-CSF), and differentiated cells were stained by tartrate-resistant acid phosphatase (TRAP) and counted. As a result, TMG1 and TMG3 were found to suppress osteoclastogenesis with IC₅₀ values of 16 and 12 μ M, respectively, whereas TMG4 exhibited no inhibition at 10 μ M, but showed cellular toxicity at 30 μ M concentration (Figure 5).

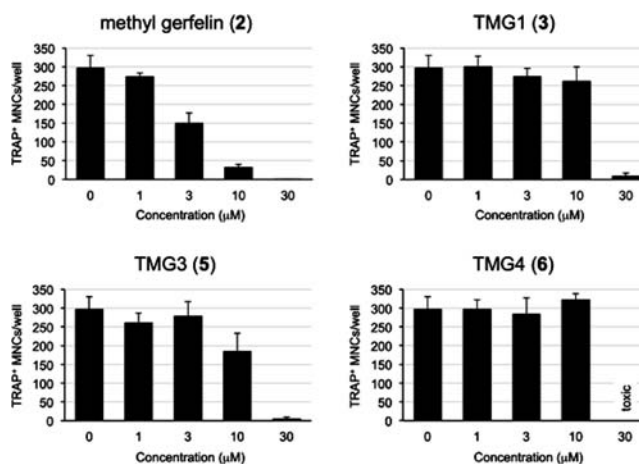


Figure 5. Osteoclastogenesis suppression of methyl gerfelin and TMG compounds.

CONCLUSION

We have prepared six TMG compounds and tested them for GLO1-inhibition activity and GLO1-binding selectivity. From the GLO1-inhibition assay, it was found that each of TMG 1–3 retained the inhibitory activity, with the activity of TMG3 being the strongest. Additional SAR experiments using synthetic intermediates confirmed the importance of the B-ring and C1-carbonyl group for GLO1 inhibition. We could conclude from these experiments that derivatization at the C6-methyl group is most suitable for use in subsequent experiments, including fluorescent labeling studies.

On the other hand, information about the binding mode of methyl gerfelin (2) toward SCP2 and SGTA proteins and information about the GLO1 selective-binding property of TMG compounds were obtained from pull-down experiments using TMG beads. That is, (1) SGTA recognizes aromatic ring(s) of methyl gerfelin (2), and (2) GLO1 and SCP2 share almost the same but not the identical area of methyl gerfelin (2).

TMG3 (5) is found to selectively bind to and inhibit GLO1. From the osteoclastogenesis inhibition assay, TMG3 (5) inhibited osteoclastogenesis comparable with, but a little stronger than, TMG1 (3). This indicated that binding of methyl gerfelin (2) to SCP2 and SGTA does not show any synergistic effects. However, a sequestration effect by either SCP2 or SGTA is sufficient to explain the results of the cell-based assay.

The TEG-scanning strategy demonstrated here is based on two different methodologies, i.e., methyl scanning and PEGylation. Methyl scanning is a method developed by Pirrung et al.,²¹ in which methylated drug derivatives are systematically synthesized and used to determine the sites of interaction between drugs and their macromolecular target(s). Although the methyl scanning strategy has been shown to work well in the design of biotinylated affinity probe for a small-molecule insulin mimic demethylasterriquinone B1,^{21,22} the probe had to be resynthesized from the beginning, so the introduction of a terminal-functionalized linker is thought to be more valuable. PEGylation²³ is originally defined as the modification of a bioactive molecule by the linking of poly(ethylene glycol) for a prolonged resistance in body and a decreased degradation by metabolic enzymes, but here we utilize oligo(ethylene glycol) as a hydrophilic linker to connect a drug and a polymer support to be used for the binding assay. Although the length and molecular weight of PEG are important for the original PEGylation strategy due to the toxicity of oligo(ethylene glycol), our cell-based assay showed that not all TMG compounds exerted cytotoxicity at the effective concentration. This indicates that a NH₂-TEG linker can be used for our purposes without any significant problem.

We believe that TEG scanning will be applicable for examining the sites of other bioactive small molecules that are recognized by multiple-binding proteins. The terminal amine group used here can be utilized for future conjugation with a reporter group such as a fluorescent dye, or a targeting agent such as an antibody. It can also be used as a handle for dimerization. Studies along these lines are now in progress.

ASSOCIATED CONTENT

Supporting Information

Experimental details of the chemical syntheses and biological assays, ¹H and ¹³C NMR spectra of synthesized compounds,

and the results of the osteoclastogenesis suppression assay. This material is available free of charge via the Internet at <http://pubs.acs.org>.

AUTHOR INFORMATION

Corresponding Author

*E-mail: nkanoh@m.tohoku.ac.jp. Phone & Fax: +81-22-795-6847.

Notes

The authors declare no competing financial interest.

ACKNOWLEDGMENTS

We thank Prof. Yoshiteru Oshima (Tohoku University) for his support, and Dr. Hiroshi Takayama (Tohoku University) for his technical assistance. This work was partially supported by a Grant-in-Aid for Scientific Research on the Innovative Area “Chemical Biology of Natural Products” from The Ministry of Education, Culture, Sports, Science and Technology, Japan (No. 23102013 to N.K.).

REFERENCES

- (1) Kawatani, M., and Osada, H. (2009) Osteoclast-targeting small molecules for the treatment of neoplastic bone metastases. *Cancer Sci.* 100, 1999–2005.
- (2) Masuya, K., and Teno, N. (2010) Small molecules for bone diseases. *Expert Opin. Ther. Pat.* 20, 563–582.
- (3) Zenitani, S., Tashiro, S., Shindo, K., Nagai, K., Suzuki, K., and Imoto, M. (2003) Gerfelin, a novel inhibitor of Geranylgeranyl diphosphate synthase from *Beauveria felina* QN22047 - I. Taxonomy, fermentation, isolation, and biological activities. *J. Antibiot.* 56, 617–621.
- (4) Zenitani, S., Shindo, K., Tashiro, S., Sekiguchi, M., Nishimori, M., Suzuki, K., and Imoto, M. (2003) Gerfelin, a novel inhibitor of geranylgeranyl diphosphate synthase from *Beauveria felina* QN22047 - II. Structural elucidation. *J. Antibiot.* 56, 658–660.
- (5) Kawatani, M., Okumura, H., Honda, K., Kanoh, N., Muroi, M., Dohmae, N., Takami, M., Kitagawa, M., Futamura, Y., Imoto, M., and Osada, H. (2008) The identification of an osteoclastogenesis inhibitor through the inhibition of glyoxalase I. *Proc. Natl. Acad. Sci. U.S.A.* 105, 11691–11696.
- (6) Kanoh, N., Kumashiro, S., Simizu, S., Kondoh, Y., Hatakeyama, S., Tashiro, H., and Osada, H. (2003) Immobilization of natural products on glass slides by using a photoaffinity reaction and the detection of protein-small-molecule interactions. *Angew. Chem., Int. Ed.* 42, 5584–5587.
- (7) Kanoh, N., Honda, K., Simizu, S., Muroi, M., and Osada, H. (2005) Photo-cross-linked small-molecule affinity matrix for facilitating forward and reverse chemical genetics. *Angew. Chem., Int. Ed.* 44, 3559–3562.
- (8) Thiede, B., Hohenwarter, W., Krah, A., Mattow, J., Schmid, M., Schmidt, F., and Jungblut, P. R. (2005) Peptide mass fingerprinting. *Methods* 35, 237–247.
- (9) Thornalley, P. J. (2003) Glyoxalase I-structure, function and a critical role in the enzymatic defence against glycation. *Biochem. Soc. Trans.* 31, 1343–1348.
- (10) Creighton, D. J., Zheng, Z. B., Holewinski, R., Hamilton, D. S., and Eiseman, J. L. (2003) Glyoxalase I inhibitors in cancer chemotherapy. *Biochem. Soc. Trans.* 31, 1378–1382.
- (11) Yamamoto, R., Kallen, C. B., Babalola, G. O., Rennert, H., Billheimer, J. T., and Strauss, J. F. (1991) Cloning and Expression of a Cdna-Encoding Human Sterol Carrier Protein-2. *Proc. Natl. Acad. Sci. U.S.A.* 88, 463–467.
- (12) Seedorf, U., Ellinghaus, P., and Nofer, J. R. (2000) Sterol carrier protein-2. *Biochim. Biophys. Acta Mol. Cell Biol. Lipids* 1486, 45–54.
- (13) Kordes, E., Savelyeva, L., Schwab, M., Rommelaere, J., Jauniaux, J. C., and Cziepluch, C. (1998) Isolation and characterization of

human SGT and identification of homologues in *Saccharomyces cerevisiae* and *Caenorhabditis elegans*. *Genomics* 52, 90–94.

(14) Miyazaki, I., Okumura, H., Simizu, S., Takahashi, Y., Kanoh, N., Muraoka, Y., Nonomura, Y., and Osada, H. (2009) Structure-affinity relationship study of bleomycins and Shble protein by use of a chemical array. *ChemBioChem* 10, 845–852.

(15) Peterson, R. T. (2008) Chemical biology and the limits of reductionism. *Nat. Chem. Biol.* 4, 635–638.

(16) Introduction on the sp^2 carbons C3, C5, C4', and C6' were not considered in this study because it would cause dramatic change to the conformation of the parent molecule.

(17) Islam, M. S., Kitagawa, M., Imoto, M., Kitahara, T., and Watanabe, H. (2006) Synthesis of gerfelin and related analogous compounds. *Biosci. Biotechnol. Biochem.* 70, 2523–2528.

(18) Hatanaka, Y., Hashimoto, M., and Kanaoka, Y. (1994) A novel biotinylated heterobifunctional cross-linking reagent bearing an aromatic diazirine. *Bioorg. Med. Chem.* 2, 1367–1373.

(19) Oray, B., and Norton, S. J. (1982) Glyoxalase-I from Mouse-Liver. *Method Enzymol.* 90, 542–546.

(20) Kanoh, N., Takayama, H., Honda, K., Moriya, T., Teruya, T., Simizu, S., Osada, H., and Iwabuchi, Y. (2010) Cleavable linker for photo-cross-linked small-molecule affinity matrix. *Bioconjugate Chem.* 21, 182–186.

(21) Pirrung, M. C., Liu, Y. F., Deng, L., Halstead, D. K., Li, Z. T., May, J. F., Wedel, M., Austin, D. A., and Webster, N. J. G. (2005) Methyl scanning: Total synthesis of demethylasterriquinone B1 and derivatives for identification of sites of interaction with and isolation of its receptor(s). *J. Am. Chem. Soc.* 127, 4609–4624.

(22) Kim, H., Deng, L., Xiong, X., Hunter, W. D., Long, M. C., and Pirrung, M. C. (2007) Glyceraldehyde 3-phosphate dehydrogenase is a cellular target of the insulin mimic demethylasterriquinone b1. *J. Med. Chem.* 50, 3423–3426.

(23) Veronese, F. M., and Pasut, G. (2005) PEGylation, successful approach to drug delivery. *Drug Discovery Today* 10, 1451–1458.